Pseudo-range measurements using OFDM channel estimation

Paul Thevenon, Olivier Julien, Christophe Macabiau, Damien Serant, Stéphane Corazza, Michel Bousquet, Lionel Ries, Thomas Grelier

Pseudo-Range Measurements Using OFDM Channel Estimation

Paul Thevenon, *TeSA-ISAE, France*
Olivier Julien, Christophe Macabiau, Damien Serant, *ENAC, France*
Stéphane Corazza, *Thales Alenia Space, France*
Michel Bousquet, *ISAE, France*
Lionel Ries, Thomas Grelier, *CNES*

BIOGRAPHY

Paul Thevenon is a PhD student in the signal processing laboratory of ENAC (Ecole Nationale de l'Aviation Civile), Toulouse, France, financed by CNES (Centre Nationale d'Etudes Spatiales) and Thales Alenia Space. He graduated as electronic engineer from Ecole Centrale de Lille in 2004 and obtained in 2007 a research master at ISAE (Institut Superieur de l'Aeronautique et de l'Espace) in space telecommunications. His current research interest is OFDM signal processing for positioning.

Olivier Julien is an assistant professor at the signal processing laboratory of ENAC. His research interests are GNSS receiver design, GNSS multipath and interference mitigation and GNSS interoperability. He received his B.Eng in 2001 in digital communications from ENAC and his PhD in 2005 from the Department of Geomatics Engineering of the University of Calgary, Canada.

Christophe Macabiau is graduated as an electronics engineer in 1992 from the ENAC. Since 1994, he has been working on the application of satellite navigation techniques to civil aviation. He received his PhD in 1997 and has been in charge of the signal processing lab of the ENAC since 2000. His research now also applies to vehicular, pedestrian and space applications, and includes advanced GNSS signal processing techniques for acquisition, tracking, interference and multipath mitigation, GNSS integrity, as well as integrated GNSS-inertial systems and indoor GNSS techniques.

Damien Serant graduated as an electronics engineer in 2008, from ENAC. He is now a PhD student in the signal processing lab of the ENAC and working on hybridization of GNSS and OFDM signals.

Stéphane Corazza is a research and development engineer in Thales Alenia Space company. He has experience in GNSS receivers design and development, LEO satellites orbit prediction and ephemeris synthesis, digital signal processing suited to radiocommunications and satellite navigation, ASIC and FPGA development for satellite digital payloads. He has received an engineering degree in 1994 in Electronics and Telecommunication in the National Institute of Applied Sciences (INSA), Lyon, France.

Michel Bousquet is a Professor at ISAE (French Institute of Higher Education in Aerospace Engineering), in charge of graduate and post-graduate programs in satellite communications and navigation. His research interests cover many aspects of satellite communications and navigation (physical and access layers, system engineering...) within the TeSA co-operative research laboratory. He has co-authored many publications in the field, including the text book "Satellite Communications Systems" published by Wiley (Fifth Edition 2010). Editor-in-Chief of the Space Communications Journal, member of the Editorial Boards of several technical journals, member of the Steering Board of the SatNEx Network of Excellence, he plays an active role in promoting R&D results from European universities and industry through active participation in Technical Committees of international conferences.

Lionel Ries is head of the Signal and RadioNavigation department of the CNES Radiofrequency sub-directorate since august 2009. He was a navigation engineer in the Transmission Techniques and Signal Processing department, at CNES since June 2000. He is one of the CBOC inventors. He graduated from the Ecole Polytechnique de Bruxelles, at Brussels Free University (Belgium) and received a M.S. degree from ISAE in Toulouse (France).

Thomas Grelier has been a radionavigation engineer at CNES since 2004. He graduated from the French engineering school Supelec and received a M.S. in electrical and computer engineering from Georgia Tech (USA). He is involved in Galileo signal processing and in the development and testing of a new RF sensor for satellite formation flying, using pulsed GPS C/A codes transmitted in S-band.

ABSTRACT

Mobile positioning using wireless telecommunication networks has been the focus of recent research as a potential, cost-effective solution for positioning a mobile user in urban environment, where the performances of Global Navigation Satellite System (e.g. availability, dilution of precision) may be reduced, while the availability of wireless telecommunication networks is important. Such research has been motivated by regulation incentives (e.g. E-911) and the explosion of location-based services.

In this paper, a method for calculating pseudo-range measurements from DVB-T/-H/-SH signals is proposed. These signals are standardized for digital TV broadcasting and uses the spectrally-efficient and multipath-resistant OFDM modulation.

The main challenge to be solved when using wireless telecommunication networks is the intense multipaths encountered in the urban propagation channel, leading to important bias in the pseudo-range measurements. The DVB-T family signals contain pilot symbols that are used for channel estimation and equalization necessary to demodulate the transmitted data, but which can also be used for pseudo-range measurement. The presented method makes use of these available pilot symbols.

The proposed method comprises 3 steps: first, an estimation of the channel impulse response is obtained by calculating the correlation of the received signal with a pilot symbol-only local replica. Then, the matching pursuit algorithm is used to coarsely estimate the delay of several taps. Finally, these initial delay estimates are used to initialize several delay-lock loops (DLL), which refine the delay estimates and track their changes.

Tracking several taps in the propagation channel is necessary to increase the chances of tracking the line-of-sight (LOS) tap in a multipath environment. Additionally, in case of Rayleigh fading usually encountered by mobile users, re-launching periodically the whole process can be useful to regain the LOS signal in case the DLL has diverged during a deep fading period.

Finally, the proposed method can be used in a modified single frequency network, where several emitters transmit the same signal in a synchronized way and on the same carrier frequency, as foreseen for the deployment of DVB-SH systems. In that case, our method would not require modifications to the receiver up to the demodulator.

This paper ends by illustrating the performances of the proposed method in AWGN, multipath and single frequency network scenarios.

INTRODUCTION

Mobile positioning with wireless networks has been the focus of many research works lately, due notably to the regulation incentive (USA's E-911, EU's equivalent E112), but also to the potential explosion of Location-Based Services, which promise to generate over $3.5 Billion yearly revenue to telecom operators by 2009 [1].

Different telecommunication networks have been investigated for positioning, with an important work of standardization at the 3GPP and ETSI for 2G and 3G mobile communication networks [2]. The performance of these positioning solutions varies a lot depending on the positioning method used, which depends on the nature of the measurements (Cell-ID, Observed Time Difference of Arrival (TDoA)) and the location of the position calculation (receiver-based or network-based). The best performance found in literature is a 1σ 2D positioning accuracy of ~60m using TDoA methods in a 3G network in urban environment [3,4]. In addition to this relatively low accuracy, positioning using 2G/3G network introduces an overall system capacity robbing required by the transfer of positioning-related information between the network elements.

Other types of telecommunication networks have been investigated, including TV or radio broadcasting network, achieving for example a 1σ 2D positioning accuracy of ~20m using a dedicated ATSC Digital TV positioning set-up in indoor environment [5].

One common issue with positioning with ground-based telecommunication networks is that the timing measurements is done on a multipath, thus creating a bias in the measurements if the line-of-sight (LOS) signal is not available [6].

In this paper, it is proposed to derive pseudo-range measurements from the channel estimation done on a DVB-SH signal used for digital television broadcast. The method includes a NLOS mitigation technique. The pseudo-range accuracy will be assessed in several propagation conditions: AWGN, multipath and Single Frequency Network channels.

The paper is organized in 6 sections. Section 1 describes the DVB-SH signal and the overview of the processes done to calculate a pseudo-range measurement. Section 2 describes the correlation process used to obtain a channel impulse response estimate. Section 3 describes the matching pursuit algorithm used to estimate coarsely the channel's tap delays. Section 4 details the delay-lock loop used for tap delay tracking. Section 5 details the strategy followed in multipath and single frequency network channel. Section 6 provides some illustrations and performances of the proposed pseudo-range measurements in different propagation channels. Finally, the article ends with a conclusion on the obtained results and the future work.

In the rest of this paper, we will use the term 'tap' to refer to a multipath in the propagation channel, as typically used by the telecommunication field..

I. DVB-SH SIGNAL OVERVIEW AND OVERALL PSEUDO-RANGE MEASUREMENT STRATEGY

DVB-T standard family overview

DVB-T (Digital Video Broadcasting - Terrestrial) is a standard created by the European Telecommunications Standards Institute to provide digital television services to fixed used in VHF or UHF band. This standard uses an Orthogonal Frequency Multiplexing (OFDM) modulation, which provides high data rates along with robustness against multipaths.
Interestingly, this standard is used as a base for the DVB-H (Handheld) and DVB-SH (Satellite to Handheld) standards which targets the mobile TV services. The latter, DVB-SH, is planned to be deployed in the S-band (2 GHz) and in Single Frequency Networks (SFN), which uses a network of synchronized emitters, with density comparable to mobile telecommunication emitters.
These two latter features - emitters' synchronization and high density - are very favorable to provide a positioning service using DVB-SH as host system, without extra (costly) infrastructure.
The rest of the article focuses on signal parameters that are specified for DVB-SH systems [11], but the proposed techniques would work with DVB-T and DVB-H systems.

OFDM principle and signal expressions

OFDM [7] consists in transmitting data symbols over several orthogonal sub-carriers, whose individual symbol rate is low enough so that the sub-carrier bandwidth is inferior to the channel's coherence bandwidth. Therefore, each sub-carrier is affected by a flat-fading distortion, which can be easily corrected using simple channel estimation techniques. The digital implementation of this modulation is achieved by the efficient FFT algorithm, allowing for large number of sub-carriers.
Additionally, a guard interval is inserted between successive OFDM symbols in order to avoid Inter-Symbol Interferences (ISI). This guard interval is used to transmit an exact replica of the end of the OFDM symbol, called Cyclic Prefix (CP).
To illustrate the OFDM principle, Fig. 1 shows an OFDM transmission block diagram.

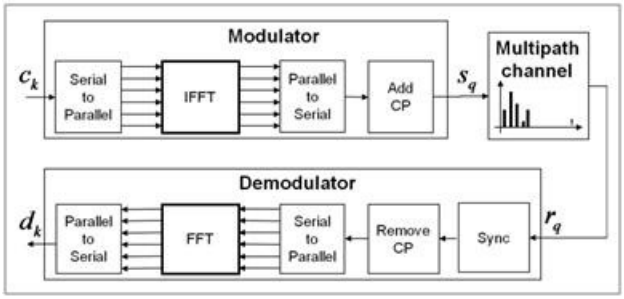

Fig. 1 - block diagram of an OFDM transmission

For a given OFDM symbol, the expression of the sent signal at the output of the modulator is

$$s_q = \sum_{k=0}^{N_{FFT}-1} c_k . e^{j2\pi \frac{kq}{N_{FFT}}} = iFFT\left[(c_k)_{k=0}^{k=N_{FFT}-1}\right](q)$$

where q is the sample index
k is the sub-carrier index
s_q is the sample value at instant q
c_k is a QAM-modulated symbol sent over sub-carrier k
N_{FFT} is the FFT size

The signal is then passed through the propagation channel. A first step of synchronization is done, in order to correct precisely the carrier frequency offset and coarsely the timing offset. This can be achieved using the Van de Beek algorithm [8], which takes advantage, through a correlation process, of the fact that the CP is a replica of the end of the OFDM symbol.
The demodulation process consists in doing the FFT of a segment of the incoming signal. The segmentation is done by placing a N_{FFT} sample-long window in order to remove the CP, and then passing these samples in a FFT. It can be noted that as long as the FFT window starts within the CP and close to the OFDM symbol true beginning, the demodulated signal will only be affected by a phase offset (and the propagation channel). Indeed, if the FFT window is placed in the CP, the resulting signal segment will have all the wanted samples, but affected by a circular permutation. This sample permutation will only affect the phase of the FFT output.
The demodulated signal expression after coarse timing synchronization is [9]:

$$d_k(\Delta\tau) = c_k H_k e^{-j2\pi \frac{k\Delta\tau}{N_{FFT}}} + n_k$$

where $\Delta\tau$ is the residual timing offset after coarse timing synchronization
$d_k(\Delta\tau)$ is the demodulated symbol on sub-carrier k, affected by the residual timing offset
H_k is the channel frequency response at sub-carrier k
n_k is a noise term affecting the symbol on sub-carrier k

To reformulate this result with words, the symbol carried by a given sub-carrier at the output of the OFDM demodulator is equal to the originally sent symbol, affected by the channel distortion on this sub-carrier. This result is illustrated in Fig. 2.
It is important to note that $H_k . e^{-\frac{j2\pi(k\Delta\tau)}{N_{FFT}}}$ is a constant flat-fading distortion over the sub-carrier bandwidth. In order to retrieve the originally sent symbol, this flat-fading

distortion can be easily corrected thanks to channel estimation techniques using pilot sub-carriers [10].
Additionally, the channel estimation technique will correct the effects of both the channel distortion and the residual timing offset. That is why only coarse timing synchronization is required in the first synchronization phase.

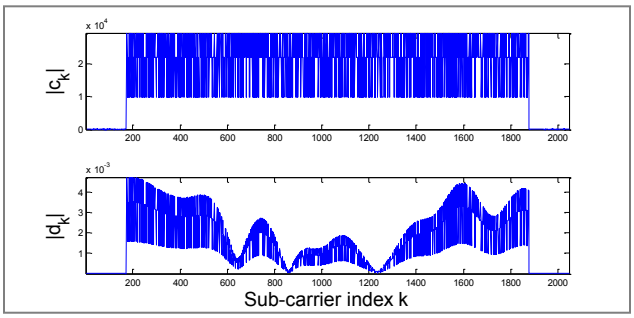

Fig. 2 - Illustration of the emitted (c_k) and channel-distorted (d_k) sub-carrier amplitude

Sub-carrier structure of the DVB-SH signals

In the DVB-SH standard [11], the symbols transmitted by the N_{FFT} sub-carriers of an OFDM symbol have different types:

- **Null** symbols, which are located on the edge of the transmission spectrum and have a zero value. They act as guard bands, used to limit the out-of-band emissions of the OFDM signal;
- **Data** symbols, which are QAM-modulated symbols (e.g. 16-QAM in Fig. 3);
- **Transmission Parameter Signaling** (TPS) symbols, carrying information about transmissions, e.g. channel coding and modulation;
- **Pilot** symbols, that are modulated by a BPSK pseudo-random sequence. Their amplitude is boosted by a factor 4/3 compared to the data or TPS symbols.

Only the latter types of symbols are used in the method presented in this paper.

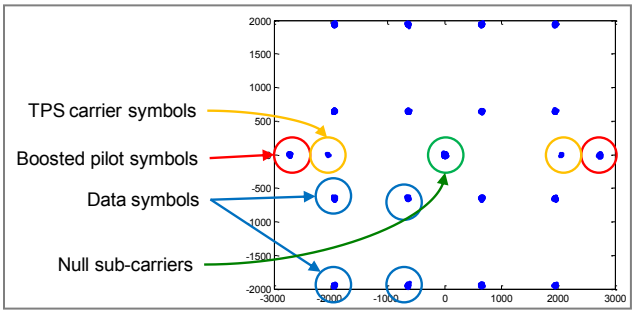

Fig. 3 - Illustration of the different types of symbols carried by the sub-carriers of one OFDM symbol.

The pilots are divided into 2 categories: fixed pilot and scattered pilots. The scattered pilots are inserted every $P = 12$ sub-carriers, with the first pilot sub-carriers taking 4 different values depending on the OFDM symbol number. The pilot sub-carrier pattern is therefore periodic, with a period equal to 4 OFDM symbols.

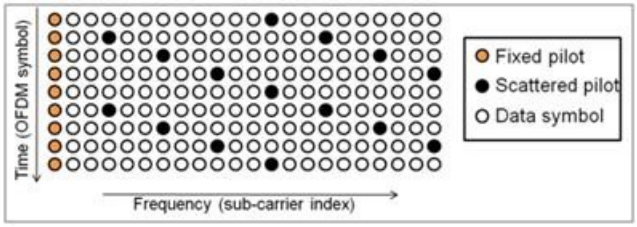

Fig. 4 - Pilot location in the DVB-T family standard

The pilots sub-carriers are used for frequency synchronization, OFDM symbol number detection and channel estimation. In our method, they will be used to obtain a CIR estimation.

Overall pseudo-range measurement strategy

The proposed strategy to obtain a pseudo-range measurement is detailed in Fig. 5 and follows these steps:

1. **Coarse timing and frequency synchronization**: achieved by using the Van de Beek algorithm [8]
2. **OFDM demodulation**
3. **Multipath delay acquisition:** coarse estimation of the channel multipaths' delay thanks to a channel impulse response (CIR) estimation. The estimated delay serves as initialization for the tracking stage;
4. **Parallel tracking:** DLLs are launched in parallel in order to refine the initial estimated delay and track possible changes in the tap delay
5. **Pseudo-range calculation:** the earliest estimated delays are used to calculate a pseudo-range measurement.
6. **Position calculation:** when the pseudo-range measurements from several emitters are available, it is then possible to calculate the mobile receiver's position.

With terrestrial propagation in urban environment, the line-of-sight (LOS) signal may be blocked or its amplitude may be very inferior to other non-LOS (NLOS) signals. Therefore, for positioning purpose, the main issue is to track a NLOS signal, thus creating an important bias (several tens or hundreds of meters) in the pseudo-range calculation.
To mitigate this issue, it is proposed to launch several DLLs in parallel in order to track several taps in the propagation channel. Then, the minimum delay value is chosen for the pseudo-range calculation, as it is the closest to the LOS path.

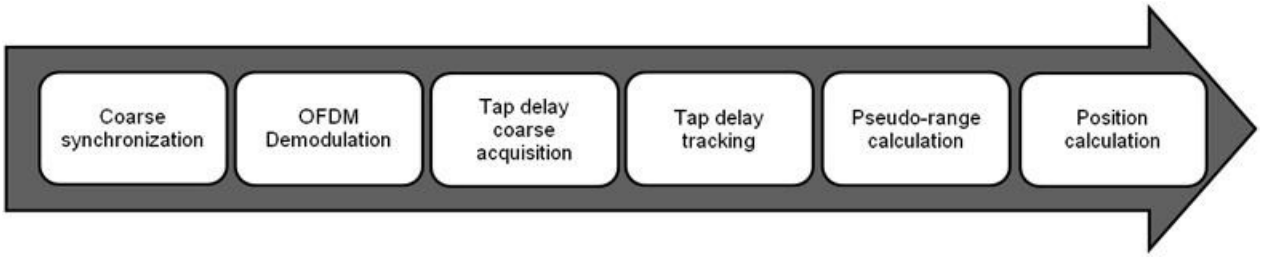

Fig. 5 - Pseudo-range measurement strategy for an OFDM receiver

II. CIR ESTIMATION BY CORRELATION WITH PILOT SUB-CARRIERS

Overview of correlator's output generation

The demodulated signal d_k is correlated (see Fig. 6) with a local replica of the expected signal created from the known pilot symbols on the scattered pilot sub-carriers and zeros elsewhere. The local replica can be delayed by a timing offset compared to the received signal named Δt. In the frequency-domain (after FFT demodulation), the local signal replica expression is

$$p_k = c_k e^{-j2\pi\frac{k\Delta t}{N_{FFT}}} \quad \text{if } k \in \mathcal{P}$$
$$p_k = 0 \quad \text{on others sub-carriers}$$

where p_k is symbol value on sub-carrier k of the local replica signal
c_k is the emitted symbol value on sub-carrier k
Δt is the delay applied to the local signal replica
$\mathcal{P}$ is the scattered pilot sub-carrier index sub-set

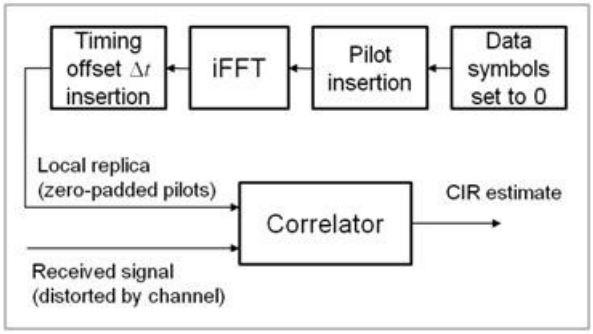

Fig 6 - block diagram of the correlation leading to the CIR estimate

Therefore, the ideal (noise-free) correlator's output expression is:

$$R(\Delta t - \Delta\tau) = \sum_{k\in\mathcal{P}} d_k(\Delta\tau)p_k^*(\Delta t)$$
$$R(\Delta t - \Delta\tau) = \sum_{k\in\mathcal{P}} c_k H_k e^{-j2\pi\frac{k\Delta\tau}{N_{FFT}}} c_k^* e^{j2\pi\frac{k\Delta t}{N_{FFT}}}$$

As the scattered pilots are evenly spaced over the sub-carriers, we can rewrite the scattered pilot sub-carrier index as

$$q \in \mathcal{P} \iff q = i.P + N_0 \text{ for } i \in [0..N_p]$$

where N_0 is sub-carrier index of the first scattered pilot. This number varies with the OFDM symbol number. $N_0 \in \{12, 3, 6, 9\} + N_{guard}$ for the DVB-T family signals.
N_{guard} is the number of null sub-carriers on the left of the transmission spectrum, which depends on N_{FFT}
N_p is the number of scattered pilot sub-carriers, which also depends on the FFT size
P is scattered pilot pattern period. $P = 12$ for DVB-SH signals.

Therefore, we can substitute the pilot sub-carrier index with this new expression:

$$R(\Delta t - \Delta\tau) = \sum_{i=0}^{N_p-1} c_k c_k^* H_{iP+N_0} e^{j2\pi\frac{(iP+N_0)(\Delta t-\Delta\tau)}{N_{FFT}}}$$

Moreover, as the pilots are BPSK-modulated symbols, $c_k.c_k^* = \sigma_p^2$, where σ_p^2 is the power of the boosted pilots.

$$R(\Delta t - \Delta\tau) = \sigma_p^2 \sum_{i=0}^{N_p-1} H_{iP+N_0} e^{j2\pi\frac{(iP+N_0)(\Delta t-\Delta\tau)}{N_{FFT}}}$$

We can notice that this expression is the N_{FFT}-point inverse discrete Fourier transform of the channel frequency response estimated on scattered pilot sub-carriers only. It is therefore directly related to the CIR. In order to illustrate this, the next paragraph takes the simple case of a single tap channel.

Case of a single tap channel

Let us apply this expression for the simple case of a single tap propagation channel: the signal is only affected by a delay τ (normalised by the sampling period), an amplitude distortion ρ and a phase distortion φ .
In this case, the channel frequency response of such channel is

$$H_k = \rho e^{j\varphi} e^{-j\frac{2\pi k\tau}{N_{FFT}}}$$

Then, using the previous expression of the correlator's output, we obtain:

$$|R(\Delta t - \Delta\tau)| = \sigma_p^2 \rho \frac{sin\left(\pi B(\Delta t - \Delta\tau - \tau)\right)}{sin\left(\frac{\pi B}{N_p}(\Delta t - \Delta\tau - \tau)\right)}$$

where $B = \frac{P.N_p}{N_{FFT}}$ is a parameter corresponding to the ratio of the sub-carriers used in the correlation and the total number of sub-carriers, the difference between the 2 being the number of null sub-carriers. It corresponds to the spectral occupation of the signal.

This function is N_p-periodic. To avoid aliasing of long delayed taps, it is preferable to decrease the periodicity of the correlation function, by increasing the number of pilots.

If it is assumed that the parameters of the multipath (ρ, τ) have remained constant over 4 OFDM symbol duration, this can be performed by doing the mean of the correlation function of 4 consecutive OFDM symbols. As the scattered pilot location is different on the 4 symbols, this is equivalent to increasing the number of pilots by a factor 4.

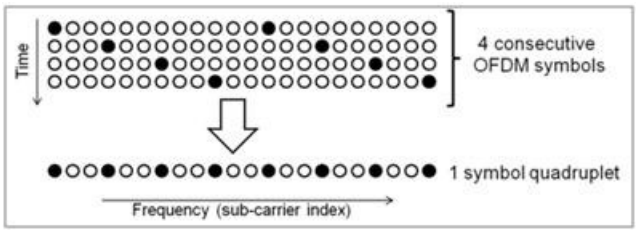

Fig 7 - Scattered pilot location of a quadruplet resulting from taking into account 4 consecutive symbols

Then, the averaged correlator's output over 4 consecutive OFDM symbols is:

$$|\bar{R}(\Delta t - \Delta\tau)| = \sigma_p^2 \rho \frac{sin\left(\pi B(\Delta t - \Delta\tau - \tau)\right)}{sin\left(\frac{\pi B}{4N_p}(\Delta t - \Delta\tau - \tau)\right)}$$

If the offset between the local replica's delay and the observed tap delay (comprising the residual timing error) is low, ie $\Delta t - (\Delta\tau + \tau) \ll 1$, the correlator's output can further be simplified by using a sinc function:

$$|\bar{R}(\Delta t - \Delta\tau)| = 4\sigma_p^2 \rho N_p \, sinc\left(\pi B(\Delta t - \Delta\tau - \tau)\right)$$

Fig. 8 depicts the correlation peak obtained by this correlation.

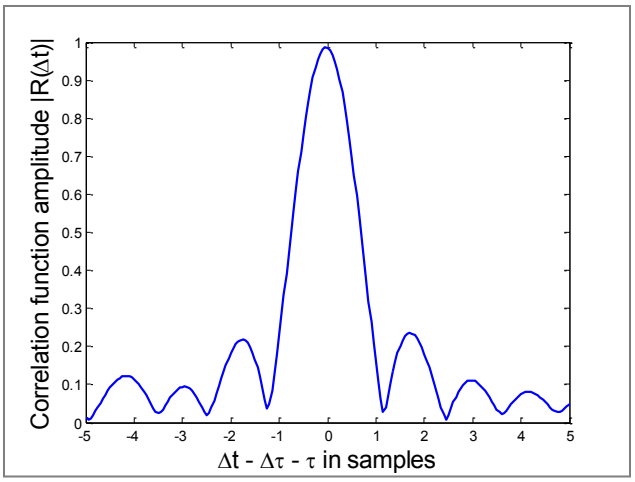

Fig 8 - Correlator's peak for a single tap

III. TAP DELAY ACQUISITION BY MATCHING PURSUIT

Matching Pursuit algorithm

From the CIR estimate obtained by a correlation done over a wide range of local replica delays (such as the one shown in Fig 8), we would like to deduce the taps' delay. This is done by using a Matching Pursuit (MP) algorithm, as proposed in [12].

The problem to solve is to find ρ_l, φ_l, and τ_l for $l \in [1..L]$ that minimize the least square residual function of the CIR estimate:

$$\hat{\rho}_l, \hat{\varphi}_l, \hat{\tau}_l = \arg \min_{\rho_l, \varphi_l, \tau_l} \sum_{k=1}^{K} \left\| \hat{h}_k - \sum_{l=1}^{L} \rho_l e^{j\varphi_l} f(k - \tau_l) \right\|^2$$

where K is the length of the estimated CIR vector
L is the number of considered multipaths
$\hat{h}_k$ is the CIR estimate at instant k
$f(k) = \frac{sin(\pi B k)}{sin\left(\frac{\pi B}{4N_p}k\right)}$ is the modeled pulse shape of the multi-path at delay k

We can rewrite this expression using matrix notation:

$$\hat{\rho}_l, \hat{\varphi}_l, \hat{\tau}_l = arg \min_{\hat{\rho}_l, \hat{\varphi}_l, \hat{\tau}_l} \left\| \hat{\mathbf{h}} - \mathbf{P}\boldsymbol{\beta} \right\|^2$$

where $\hat{\mathbf{h}} = \left[\hat{h}_1, \hat{h}_2, \dots, \hat{h}_K\right]^T$ is the vector of the CIR estimates
$\mathbf{P} = [\mathbf{P_1}, \mathbf{P_2}, \dots, \mathbf{P_L}]$ is a KxL matrix containing the pulse samples for each considered tap delay
$\mathbf{P_l} = [\mathrm{f}(1 - \tau_l), \mathrm{f}(2 - \tau_l), \dots, \mathrm{f}(K - \tau_l)]^T$ is the pulse sample of the l-th delay
$\boldsymbol{\beta} = [\rho_1 e^{j\varphi_1}, \rho_2 e^{j\varphi_2}, \dots, \rho_L e^{j\varphi_L}]^T$ is the vector of the complex amplitude of the taps

The matching Pursuit algorithm permits to find only the delays $\hat{\tau}_l$. The principle is to find iteratively the most probable delay of a pulse from the CIR estimates. After each iteration, the CIR vector is corrected by removing the pulse of the retained path and a new delay is estimated.

We initiate the CIR estimate vector $\hat{\mathbf{h}}_\mathbf{0} = [\hat{h}_1, \hat{h}_2, \dots, \hat{h}_K]$
For each step i, the following operations are done:

1. The most probable instant is found:
$$\hat{\tau}_i = arg\,\max_l \frac{\left|\mathbf{P_l^H}.\hat{\mathbf{h}}_\mathbf{i}\right|^2}{\left\|\mathbf{P_l^H}\right\|^2}$$
2. The CIR estimate is corrected by the pulse centered on $\hat{\tau}_i$:
$$\hat{\mathbf{h}}_{\mathbf{i+1}} = \hat{\mathbf{h}}_\mathbf{i} - \frac{\mathbf{P_l^H}.\hat{\mathbf{h}}_\mathbf{i}}{\left\|\mathbf{P_l^H}\right\|^2}.\mathbf{P_l}$$

These steps are looped until a given number of tap delays have been found or until $\left\|\hat{\mathbf{h}}_\mathbf{i}\right\| < \varepsilon$

Tap amplitude thresholding

The main drawback of this algorithm is its false alarm rate, due to a false peak detection in the channel estimation, that can be due to thermal noise.
This type of error can be mitigated by limiting the search domain around the taps' expected delays, and by excluding taps with low amplitude.

Assuming that the estimated delay $\hat{\tau}_l$ is close to the true observed tap delay $\Delta\tau + \tau_l$, an estimation of the tap's amplitude can be obtained by taking the correlation at the estimated delay:
$$\hat{\rho}_l = \frac{|\bar{R}(\hat{\tau}_l - \Delta\tau)|}{4N_p\sigma_p^2}$$

The retained delays for the tracking step are:
$$\{\hat{\tau}_l, \hat{\rho}_l > threshold\}$$

The threshold has been chosen empirically to a value equal to -30 dB below the noise floor level for the signal parameters summarized in Table 2.

IV. TAP DELAY TRACKING BY DELAY-LOCK LOOP

Discriminator's output expression

In order to refine the delay estimation obtained by MP and track the variations of the delay, a delay-lock loop (DLL) is used. One DLL is launched for each tap that was above the amplitude threshold during the acquisition step.
The studied DLL has been proposed by [13] and makes use of 3 correlator's outputs:

- a 'prompt' correlator, where the local replica is delayed by a previous delay estimate (either from the acquisition step or from the previous estimate during the tracking phase)
- an 'early' correlator, where the local replica is further delayed by $\delta/2$
- a 'late' correlator, where the local replica is further delayed by $-\delta/2$

The parameter δ is called the discriminator's spacing and is normalized by the sample duration. It is chosen equal to 1.

The absolute value of the different correlators is given by the following expressions:
$$\left|R^{prompt}(\varepsilon)\right| = 4\sigma_p^2\rho N_p\, sinc(\pi\varepsilon B)$$
$$\left|R^{early}(\varepsilon)\right| = 4\sigma_p^2\rho N_p sinc\left(\pi\left(\varepsilon - \frac{\delta}{2}\right)B\right)$$
$$\left|R^{late}(\varepsilon)\right| = 4\sigma_p^2\rho N_p sinc\left(\pi\left(\varepsilon + \frac{\delta}{2}\right)B\right)$$
where $\varepsilon = \Delta t - (\Delta\tau + \tau)$ is the error between the local replica delay Δt and the delay to be estimated $(\Delta\tau + \tau)$

The discriminator used in this DLL is a normalized $|E|^2$-$|L|^2$ one. Its expression is:
$$D(\varepsilon) = \frac{\left|R_l^{early}(\varepsilon)\right|^2 - \left|R_l^{late}(\varepsilon)\right|^2}{|R^{prompt}(\varepsilon)|^2}$$
$$= \frac{sinc\left(\pi\left(\varepsilon - \frac{\delta}{2}\right)B\right)^2 - sinc\left(\pi\left(\varepsilon + \frac{\delta}{2}\right)B\right)^2}{sinc(\pi\varepsilon B)^2}$$

In order to normalize the discriminator's linear zone, we have to divide $D(\varepsilon)$ by the slope of $D(\varepsilon)$ around $\varepsilon = 0$.
$$D_{norm}(\varepsilon) = \frac{D(\varepsilon)}{K_{norm}}$$

where,
$$K_{norm} \triangleq \lim_{\varepsilon\to 0}\frac{D(\varepsilon)}{\varepsilon} = \frac{1 - \frac{\delta}{2}\pi B\sin(\pi B\delta) - \cos(\pi B\delta)}{\pi^2 B^2\frac{\delta^3}{16}}$$

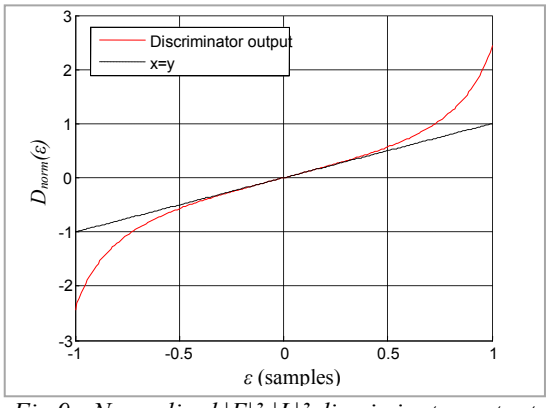

Fig 9 - Normalized $|E|^2$-$|L|^2$ discriminator output

Loop filter

The discriminator's output at instant l is used to update the estimated delay of the tap computed at the previous instant $l-1$.
In order to reduce the noise in the loop, a 2nd order loop filter is used, according to [14].

It should also be mentioned that clipping the DLL's output has been implemented, thus limiting the DLL divergence in case of important discriminator output value, either due to a bad normalisation conditions (prompt correlator close to zero due to thermal noise) or to the presence of strong taps a few samples away.

Simulated performances of the DLL

We have simulated the performance of the DLL in a single-tap Gaussian channel. The parameters in this simulation are summarized in Table 2. Fig 10 shows the standard deviation of the error for different SNR values. The SNR value is taken at the input of the demodulator.

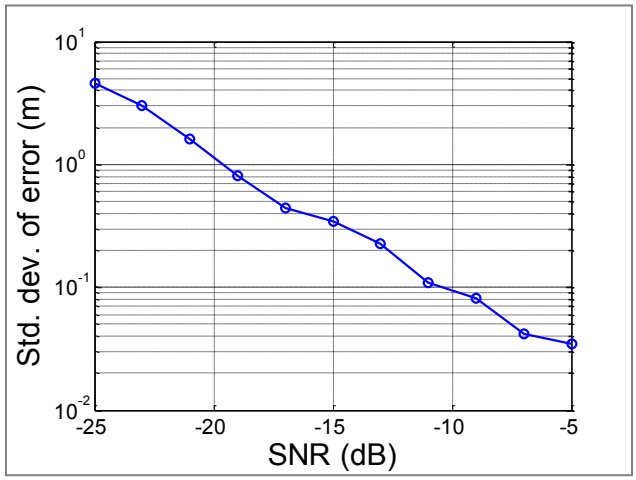

Fig 10 - Standard deviation of the error vs SNR

We observe promising results for the tracking of single-taps, even for low SNR. This is important in order to be able to track the taps even during a deep fading phase in multipath channels or for remote emitters in SFN channel.

V. THE MULTIPATH CHANNEL CASE

TU-20 channel

The propagation channel typically encountered in the urban environment between a terrestrial emitter and a receiver is usually modeled by several taps whose amplitude is varying with a Rayleigh distribution and a Jake's spectrum [15]. Such model is proposed for S-band transmission in the UMTS standard [16].

Table 1

Tap number	Delay (µs)	Avg relative power (dB)	Doppler Spectrum
1	0	-5.7	Jake
2	0.217	-7.6	Jake
3	0.512	-10.1	Jake
4	0.514	-10.2	Jake
5	0.517	-10.2	Jake
6	0.674	-11.5	Jake
7	0.882	-13.4	Jake
8	1.230	-16.3	Jake
9	1.287	-16.9	Jake
10	1.311	-17.1	Jake
11	1.349	-17.4	Jake
12	1.533	-19.0	Jake
13	1.535	-19.0	Jake
14	1.622	-19.8	Jake
15	1.818	-21.5	Jake
16	1.836	-21.6	Jake
17	1.884	-22.1	Jake
18	1.943	-22.6	Jake
19	2.048	-23.5	Jake
20	2.140	-24.3	Jake

This means that, if we use this model, although the tap delays are constant in time, their amplitude may vary a lot and may disappear during deep fading periods (Fig. 11).

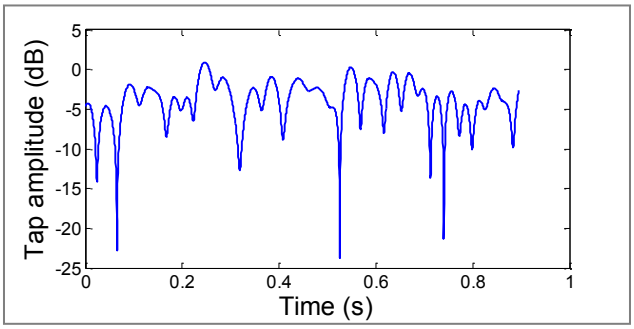

Fig 11 - Illustration of tap amplitude variation for a mobile user (10 km/h)

Moreover, as we see in Fig 12, the peak amplitude in the CIR can be at a later instant than LOS path delay. This means that the LOS tap's amplitude will be inferior to the amplitude of later taps, which may create a bias in the pseudo-range calculation.

Therefore, it is interesting to periodically launch a new acquisition phase and the ensuing DLLs in order to increase the probability to track the earliest tap, which would be the closest to the LOS ray.
In order to reduce the number of running DLLs, several DLL-stopping schemes are implemented:

- new DLLs are not launched if the delay obtained by the Matching Pursuit algorithm is too close to an already running DLL
- If 2 DLLs have converged towards the same delay (within a range of 1 sample for a duration

equivalent to the convergence constant of the DLL), one of them is stopped.
- If the amplitude associated to the tracked tap is too low, the DLL is stopped.

In Fig. 13, the true tap delays are represented in dotted line, with the LOS ray being the earliest. The colored lines are the estimated delays. The DLL parameters are described in Tab. 3.
The number of running DLLs in this example converges toward 15.

Despite the low loop noise bandwidth used in the simulation ($B_l = 10$ Hz), we observe that the estimated delays have a very fast variation over time. One reason could be the presence of strong nearby multipaths (sometimes +15 dB, see Fig. 12) affecting the discriminator's output.

At a given instant, the chosen ToA measurement is the minimum of the estimated delays.

Modified Single Frequency Network (SFN) channel

Modification to a SFN was proposed in [17] to permit the discrimination of emitters in the CIR estimate. The modification consists in introducing artificial delays between neighboring emitters, so that the taps from different emitters do not overlap. Interestingly, this modification would not require modifications in the receiver for the telecommunication part, if the right OFDM signal parameters are chosen.

The same strategy can be applied as in the previous single emitter multipath channel. The main difference is that the amplitude of the taps coming from different emitters may vary a lot. Also, in order to avoid the iso-delay zone issue presented in [17], we have to keep only the taps coming from nearby emitters.
Therefore, the amplitude threshold for keeping a delay during acquisition and launching DLLs shall be adapted to this case. The new tap amplitude threshold has been chosen empirically at -35dB below the noise floor.

Once we have obtained the delay estimates, we have to group the delays in clusters, each cluster being associated to one emitter.
To do this, a classical clustering algorithm [18] is applied, by separating clusters whose weighted centroid delays are separated by more than a threshold depending on the single-emitter channel maximum delay (2.14 µs for the TU-20 model).

Fig. 15 shows the same channel estimates as in Fig. 14 after clustering. Then, the minimum delay of each clustered delay estimates is chosen for the pseudo-range calculation.

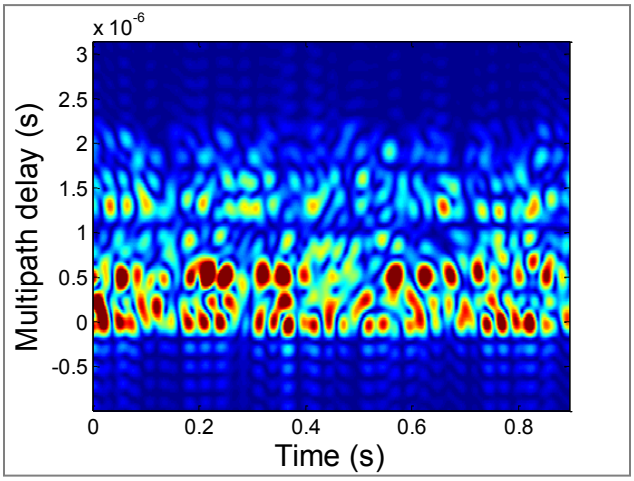

Fig 12 - Illustration of CIR evolution (10 km/h)

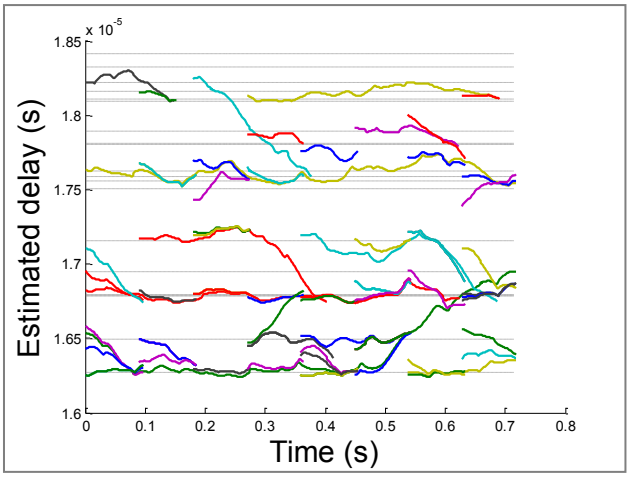

Fig 13 - Illustration of true (dotted, gray) and estimated (colored, plain) tap delays with periodic MP delay acquisition (every 90 ms)

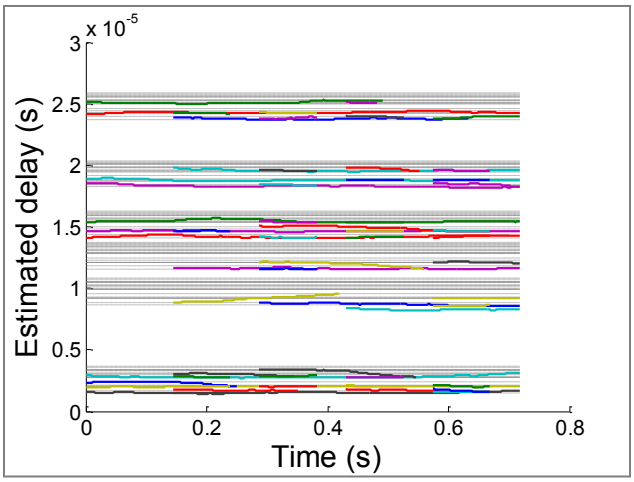

Fig 14 - Estimated delays in a SFN. Several groups of delays appear, each one associated to a given emitter.

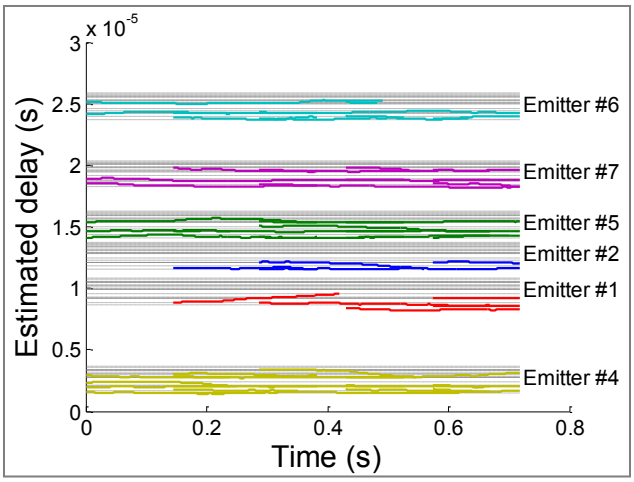

Fig 15 - Estimated delays in a SFN after clustering.

VI. SIMULATION AND PERFORMANCES

The DVB-SH signal parameters that were used in the presented simulations are presented in Table 2.

Table 2

Parameter	Value
FFT size - N_{FFT}	2048
CP length	1/4
Signal bandwidth	5 MHz
Length of simulation	5000 OFDM symbols
Symbol duration - T_{symb}	448 µs
Sample duration - T_{samp}	175 ns

Single emitter TU-20 channel

The proposed method has been evaluated in a single emitter TU-20 propagation channel [16]. In order to take realistic transmission conditions, we have applied power correction to the signal and noise coming from reference budget link [19] and pathloss model [20] for a DVB-SH system. The parameter used in this simulation are given in Table 3. The resulting average aggregate SNR is 21.6dB.

Table 3

Parameter	Value
Link budget and propagation channel	
Emitter EIRP	23.2 dBW
Emitter's height	23 m
Receiver's antenna gain	-1 dB
Receiver's noise factor	5 dB
Receiver's speed	10 km/h
Receiver's height	1.5 m
Noise bandwidth	4.758 MHz
Pathloss model	COST 231 Wallfisch-Ikegami
Carrier frequency	2.2 GHz
Roof height	20 m
Building separation	40 m
TX / RX distance	600 m

Matching Pursuit parameters	
Amplitude threshold	-30 dB
Delay interval of CIR estimation	34.5 µs
Pulse matrix time resolution	1/8 sample
DLL parameters	
Noise bandwidth	10 Hz
Integration time	4 T_{symb} = 1.792 ms
$\|E\|^2$-$\|L\|^2$ discriminator spacing	1 sample
DLL order	2

Fig. 18 shows the CDF of the estimated error for different interval length between 2 delay acquisition.

For every interval value, the distribution of the error is bi- or tri-modal, with a peak value around a 0m error, and 2 others toward -80m and a positive one. The negative error peak is due to bad initial estimation of the delay by the Matching Pursuit algorithm in the acquisition phase, while the positive peak corresponds to instants when the LOS ray suffers from fading and the DLL is attracted towards later taps.

It should also be mentioned that the number of operations for pseudo-range calculation increases as the interval value decreases. Indeed, the MP algorithm requires the calculation of the correlation over a wide range of points (several hundred), while the DLL only requires the correlation on 3 points.

The best value for interval between 2 delay acquisitions is chosen to be 80 symbol quadruplets.

Modified SFN channel

The SFN channel is modeled by creating several independent TU-20 channels, each associated to one emitter, which are then added with an amplitude and

delay correction calculated from the distance between the emitter and the receiver.
Additionally, artificial transmission delay between neighboring emitters are introduced to each channel, as proposed in [17].
No shadowing was simulated.

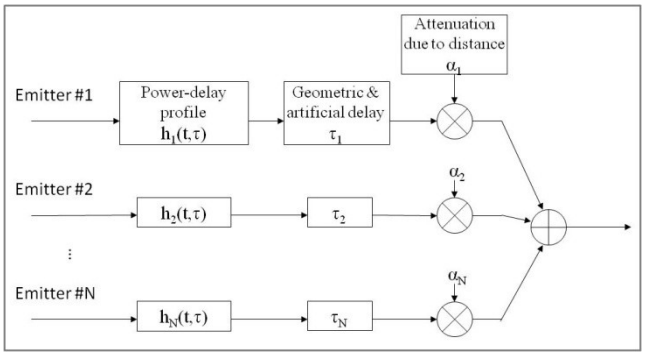

Fig 16 - SFN simulation principle

The parameters of the Matching Pursuit have changed, in order to account for the longer CIR to be estimated and weaker tap amplitude (See Table 4).

Table 4

Matching Pursuit parameters (SFN simulations)	
Amplitude threshold	-35 dB
Delay interval of CIR estimation	54 µs
Pulse matrix time resolution	1/8 sample
Clustering parameters	
Method	Weighted Center of Mass
Clustering threshold	1.8 µs

The considered scenario is depicted in Fig. 17. The SFN deployment is described in Table 5 and was considered in order to provide a minimum average SNR of 10 dB over the whole service coverage.

Table 5

Modified Single Frequency Network parameters	
Emitter separation	1 km
Minimum SNR in service coverage	10 dB
Artificial delay step	4 µs
Artificial delay reuse factor	7

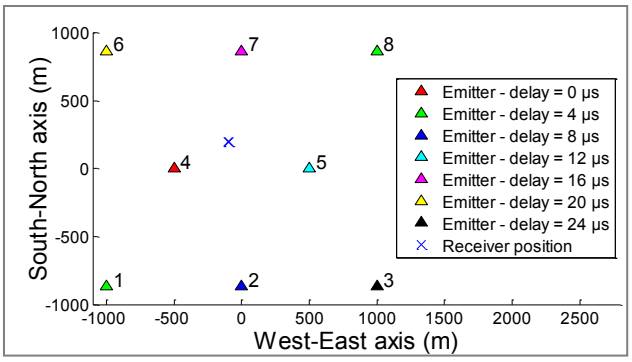

Fig 17 - emitters and receiver's location for the 8-emitter SFN simulations

Table 7 shows the pseudo-range measurement's performances for each emitter, ranked by distance.

As expected the pseudo-range accuracy for farther emitters (1, 2 and 6) is degraded compared to the pseudo-range accuracy of nearer emitters (4, 5 and 7), due to worse SNR conditions.
The mean pseudo-range error can reach several tens of meters for remote emitters, which would create a bias in the final position estimate. However, such strongly biased measurements could be detected and excluded by using outlier detection techniques [21].

CONCLUSION AND FUTURE WORK

In this paper, a pseudo-range measurement method for OFDM signals is presented and applied to DVB-SH signals. The method uses the pilots already present in OFDM signals to obtain a channel impulse response and calculate the ToA of a signal. In case of multipath propagation channels, several taps can be detected and tracked in order to mitigate the risk of measuring a NLOS, biased ToA.

The method has been tested in AWGN, multipath and single frequency propagation channel, with an illustration of the performances. The performances in multipath and SFN channels give a mean pseudo-range error below 20m, mainly due to the intense multipaths. The distribution of errors shows bi- or tri-modal distributions, the main peak being centered close to 0 and each additional peak corresponding to either a phase of convergence of a badly-initialized DLL or a loss of the LOS signal.

Future work will try to characterize the Matching Pursuit and DLL performances and robustness to multipath, especially in low SNR conditions. It will also be interesting to observe the behavior of the proposed method with more realistic propagation channels, by using either more elaborate channel models or a record of real signals.

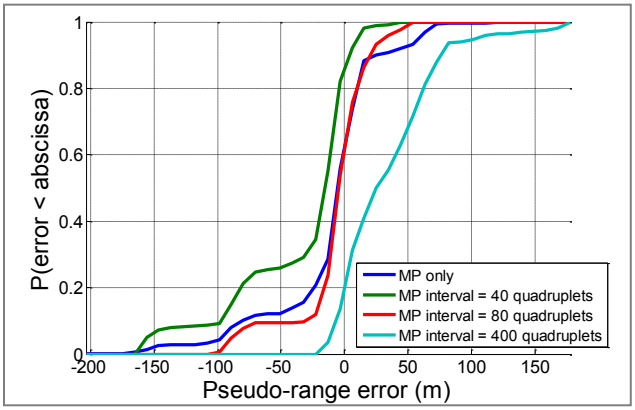

Fig 18 - CDF of error for different interval between 2 MP acquisition

Table 6

Interval value (quadruplets)	Average error (m)	Standard deviation of error (m)
0	-6.4	43.2
40	-4.7	31.1
80	7.3	17.7
400	38.3	38.9

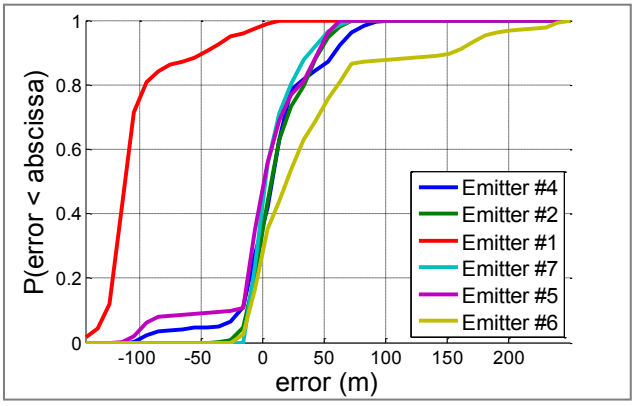

Fig 19 - CDF of error for each tracked emitter of the SFN

Table 7

Emitter	True distance (approx.)(m)	Average error (m)	Standard deviation of error (m)
4	450	13.7	34.1
5	630	4.9	37.3
7	675	12.8	18.9
2	1070	16.6	22.0
6	1120	43.2	59.9
1	1395	-98.1	31.9

ACKNOWLEDGMENTS

This work has been funded by the French space research agency (Centre National d'Etudes Spatiales) and Thales Alenia Space, France.

REFERENCES

[1] Alcatel Location Based Solutions – White Paper. 2006. Available at http://www.liaison-project.eu/download/2006-11-15%20LBS.pdf

[2] ETSI TS 123 271 - Digital cellular telecommunication system (Phase 2+); Universal Mobile Telecommunications System (UMTS); LTE; Function stage 2 description of Location Services (LCS) (3GPP TS 23.271). 2009.

[3] Ludden B, Lopes L. Cellular based location technologies for UMTS: a comparison between IPDL and TA-IPDL. In: Vehicular Technology Conference Proceedings. 2000 IEEE 51st. vol. 2; 2000. p. 1348-1353 vol.2.

[4] Porcino D. Performance of a OTDOA-IPDL positioning receiver for 3GPP-FDD mode. In: 3G Mobile Communication Technologies, 2001. Second International Conference on; 2001. p. 221-225.

[5] Rabinowitz M, Spilker JJ. A new positioning system using television synchronization signals. In: IEEE Transactions on Broadcasting, Vol. 51, No. 1. (2005), pp. 51-6; 2005.

[6] Wylie MP, Holtzman J. The non-line of sight problem in mobile location estimation. In: Universal Personal Communications, 1996. Record., 1996 5th IEEE International Conference on. vol. 2; 1996. p. 827-831 vol.2.

[7] Bingham JAC. Multicarrier modulation for data transmission: an idea whose time has come. Communications Magazine, IEEE. 1990; 28(5):5-14.

[8] van de Beek JJ, Edfors O, Sandell M, Wilson SK, Borjesson PO. On channel estimation in OFDM systems. In: Vehicular Technology Conference, 1995 IEEE 45th. vol. 2; 1995. p. 815-819 vol.2.

[9] Morelli M, Kuo CCJ, Pun MO. Synchronization Techniques for Orthogonal Frequency Division Multiple Access (OFDMA): A Tutorial Review. Proceedings of the IEEE. 2007;95(7):1394-1427.

[10] Chiueh TD, Tsai PY. OFDM Baseband Receiver Design for Wireless Communications. 1st ed. Wiley; 2007.

[11] ETSI EN 302 583 - Digital Video Broadcasting (DVB); Framing Structure, channel coding and modulation for Satellite Services to Handheld devices (SH) below 3 GHz. 2008.

[12] Cotter SF, Rao BD. Sparse channel estimation via matching pursuit with application to equalization. Communications, IEEE Transactions on. 2002;50(3):374-377.

[13] Yang B, Letaief KB, Cheng RS, Cao Z. An improved combined symbol and sampling clock synchronization method for OFDM systems. In: Wireless Communications and Networking Conference, 1999. WCNC. 1999 IEEE; 1999. p. 1153-1157 vol.3.
[14] Stephens SA, Thomas JB. Controlled-root formulation for digital phase-locked loops. Aerospace and Electronic Systems, IEEE Transactions on. 1995;31(1):78-95.
[15] Jakes WC. Microwave Mobile Communications. Second revised edition ed. Wiley; 1994.
[16] ETSI TR 125 943 v6.0.0 - Universal Mobile Telecommunications System (UMTS); Deployment aspects (3GPP TR 25.943). 2004.
[17] Thevenon P, Julien O, Macabiau C, Serant D, Ries L, Corazza S, et al. Positioning principles with a mobile TV system using DVB-SH signals and a Single Frequency Network. In: Digital Signal Processing, 2009 16th International Conference on; 2009. p. 1-8.
[18] Jain AK, Dubes RC. Algorithms for Clustering Data. Prentice Hall College Div; 1988.
[19] Chuberre N, Bodevin F, Courseille O, Duval R, Dussauby E, Selier C. Unlimited Mobile TV. In: ASMS 2006
[20] Digital Mobile Radio Towards Future Generation Systems – COST 231 Final Report. 1993.
[21] Chen PC. A non-line-of-sight error mitigation algorithm in location estimation. In: Wireless Communications and Networking Conference, 1999. WCNC. 1999 IEEE; 1999. p. 316-320 vol.1.